Fatigue Analysis of a Cracked Shaft: a Finite Element Modeling Approach

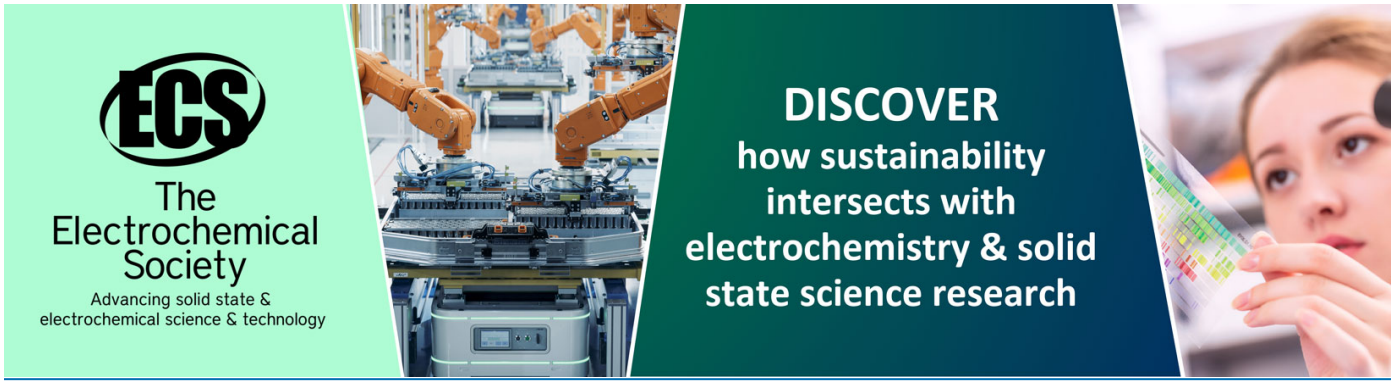

FATIGUE ANALYSIS OF A CRACKED SHAFT: A FINITE ELEMENT MODELING APPROACH

G. Thinesshwaran[1], M.M.N. Husnain[1], M.R.M Akramin[1], M.S. Shaari[1]

and Akiyuki Takahashi[2]

[1]Faculty of Mechanical & Automotive Engineering Technology,
Universiti Malaysia Pahang Al-Sultan Abdullah, 26600 Pekan, Pahang, MALAYSIA.

[2]Tokyo University of Science, 2641 Yamazaki, Noda, Chiba, 278-8510, JAPAN

Abstract. Shafts are typically used in sophisticated mechanisms and machinery which highly depend on shafts for rotatory motion which could lead to the failure. In today's contemporary, damages caused by cracking on mechanical components and structures have increased, causing crack and structural failure. The failure could be examined by the calculation of stress intensity factor (SIF). Once the shaft reaches the critical SIF (SIF_{IC}), the flaw is initiated and has a potential to propagate upon loading. Typically, the flaw would spread in many patterns and tenders to the formation and initiation of different types of cracks. Thus, the objective of this research work is to analyse fatigue cracked shafts. Prediction of crack growth via SIF calculation. SIF is usually adapted to predict the stress intensity near the crack tip where crack propagation occurs. Thus, SIF is used to study and analyse the cracked surface in relation to crack initiation and propagation. The SIF is calculated through finite element method (FEM) since the FEM is capable simulating complex geometry. The SIF is calculated based on the deformation in FEM calculation. The results show the predicted crack propagation and SIF calculation. It is crucial to study the resistance of cracked shafts towards cyclic loading for maintenance preceding and retirement of the structure.

Keywords: Surface Crack; Finite Element; Stress Intensity Factor; Shaft

1 INTRODUCTION

Cracking is a phenomenon also known as damage caused by residual stress on a material that can quickly occur on materials due to influences of several factors. Factors that influence cracking include corrosion, fatigue, pressure, applied loads, vibration, and more [1], [2]. Cracks on a surface not only reduce the strength of the material through the deduction in the cross-section thickness but also readily propagate the material through stress concentration at the tip under cyclic loading [3]. Crack formation on engineering components and structures occurs due to continuous stress on the subject especially on the rotating structure like shaft [4]–[6].

Thus, the shafts that are condoned to undergo cyclic loading over a prolonged period which may lead to metal fatigue [7]. The most sophisticated mechanisms and machines existing in this world have shafts functioning, which hands the mechanisms to function.

Like other mechanical components, shafts also could be affected by the cracking phenomenon, which leads to metal fatigue. When shafts are continuously subjected to various types of force and loadings while in rotation, the metals often undergo elastic deformation, which could lead to metal fatigue [8]. Metal fatigue is a phenomenon that weakens the material due to continuous and cyclic loading over a period of time. Fatigue advocates mechanical failure and structural damages [9], which may damage the materials progressively due to constant loading. Metal fatigue causes crack growth and crack propagation, which could lead to permanent deformation [10]. When shafts are subjected to constant and rapid metal fatigue, it causes the shaft to be under continuous stress/pressure, which advocates to metal fracture [11]. Over time, when the shaft reaches fracture, the propagation of cracks could be observed, leading to permanent fracture [12]. Thus, the study of the SIF of shafts is essential to understand the fatigue life of the shafts [13], which could also indicate their life span [14]. The study of metal fatigue revolves around fracture mechanics under the Linear Elastic Fracture Mechanics concept [15].

The response from the SIF (ability to withstand the loading) enables engineers/workers to render the correct shaft to any mechanical mechanism or machine [16]–[18]. The study of SIF is also necessary to consider fatigue crack propagation and fracture among the possible failure modes [19]. The study of cracked surfaces is imperative because it has a major significant influence on the mechanical characteristics of an object [20]. Moreover, the study of SIF on cracked surfaces also tenders the stress intensity which subdues it [21]. The outcome could be used to further the scope of manufacturing a more splendid shaft type that could withstand higher residual stress. Hence, for this research work, an analysis of the cracked shaft under cyclic loading is embarked. The analysis obtained from this study further helps to improve the understanding of the SIF on a shaft due to residual stress, which could determine its ability to withstand pressure over a period of time [22], [23]. An outcome could be derived, and a solution could be drawn after the analysis regarding the usage of the shaft upon the subjection of cyclic loading. With the derived outcome, one can expedite their knowledge on suitable uses of shafts based on the stress situation which is subjected to the shaft in real-life [24].

Thus, the main objectives of the study is to investigate the crack growth propagation of the cracked shaft, upon the subjection of stresses by cyclic loading and to analyse the Stress

Intensity Factor (SIF) of a cracked surface on a shaft which is subjected to cyclic loading. Henceforth, the results of this study will be expediated and revolve around these trusses which is the pillar of this study.

2 METHODOLOGY

The shaft is adapted from a crane trolley wheel of 4140 Alloy Steel, subjected to carry a crane of 25 tonnes. Crane trolley wheels are mainly used in heavy lifting machine mechanisms that are used to locomote objects from one place to another. Crane trolley wheels are fixed to the lifting machine mechanisms to move the machine from one place to another. Crane trolley wheels use a variety of crafts made from various materials and precisely regulate the quench and temper temperatures to get the desired metallographic structure and mechanical properties. Table 2.1 shows the material properties for 4140 Alloy Sseel.

However, while the shafts are continuously subjected to various types of force and loadings while in rotation, the metals tend to undergo elastic deformation, which could lead to metal fatigue. Metal fatigue then causes crack growth and crack propagation, which could lead to permanent deformation or metal failure. The metal fatigue causes the shaft to be fractured and damaged, which tenders the shaft to not function properly due to its lowered life span. A cracked shaft could have a disastrous and deadly impact on the dynamic behaviour of rotating structures and seriously harm rotating gear. Such damages can cause the system to collapse completely, incurring expensive downtime costs. As a result, condition monitoring systems are necessary for dynamic rotor machinery to operate safely and economically.

The shaft in Figure 2.1 depicts the cracked surface of the shaft of the crane trolley wheel which has reached metal fatigue. In conjunction, the analysis of the below shaft is done in the S-version Finite Element Method (S-FEM) software tantamountly based on the state of affairs which the shaft has undergone. The analysis obtained from the software is used to enhance the research.

TABLE 2.1 MATERIAL PROPERTIES FOR 4140 ALLOY STEEL [25].

Properties	Value
Modulus of elasticity, *E*	210 GPa
Poison's ratio	0.3
Paris *C*	1.0×10^{-10}
Paris *n*	2.08

Figure 2.1 The visual examination of the shaft failure point.

The shaft from Figure 2.1 is a part of a mechanical device that conveys rotational motion and power to external components like gears and pulleys. The crane trolley wheel which needs rotational motion to function also have shafts. The main objective of this shaft is to convey torque from an external source to the differential, which then transmits this torque to the wheels in order to move the vehicle. For the crane trolley wheel, the shaft is locked to the bearings of the wheel where it holds the bearing firmly while rotation. The end of the bearing is fixed to the motor which provides rotatory motion to the shaft. The rotation of shafts causes the wheel to rotate and provide motion to the trolley. The state of affairs of the shaft in this study is depicted in Figure 2.2.

S-FEM software is used to analyse the crack formation and propagation on a 3-Dimensional model. The S-FEM software is suitable for large-scale simulations like complex crack analysis problems. The S-FEM software is an entirely automated system for simulating the growth of fatigue cracks. While using the S-FEM software, a local mesh needs to be generated and the crack growth and propagation simulation is analysed. However, using the S-FEM analysis, a methodology for enhancing the accuracy of finite element calculations in regions with

unacceptable errors has also been developed. The S-FEM software improves the resolution of the analysis by superimposing a mesh of higher-order hierarchical elements (hexahedral mesh generation) on top of the original mesh, which makes the denouement of the analysis to be more precise.

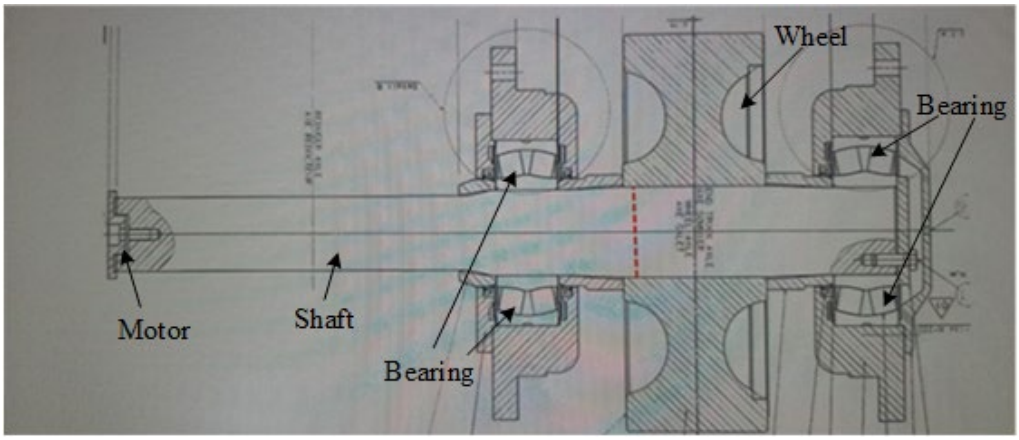

Figure 2.2 The depiction of shaft in the crane trolley wheel

Critical equations for fatigue crack life analysis are also developed using the stress intensity factors (SIF) equations and the energy release rate for the crack model. The derivation of the S-FEM formulation is discussed in further detail in the following section. In the formulation, the concept and methods of 3D analysis in the S-FEM software will be emphasised by continuing the finite element analysis on the mesh-generated shaft. The process continues with the generation of global mesh on the generated shaft. Mesh generation is the process of dividing a continuous geometric space into separate geometrical and topological cells.

In Figure 2.3, the meshes in the S-FEM software are generated. Mesh generation is essential for the accurate capturing of the input domain geometry.

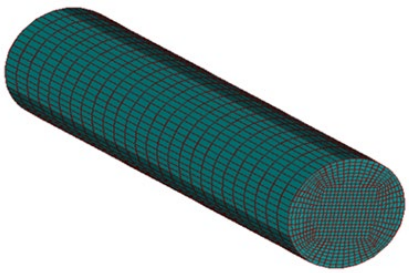

Figure 2.3 The depiction of the global mesh generated shaft in s-version finite element method software.

Then, the boundary conditions are inserted on the mesh-generated shaft of the crane wheel trolley based on the real-life situation. The boundary conditions affect the stress distribution acting on the shaft when the load is inserted. One side of the shaft is set at a fixed position for this shaft. Then, the loads are substituted into the mesh-generated shaft. In Figure 2.4, the three loadings were inserted on the constructed mesh-generated shaft in the S-FEM software. Firstly, two-point loads were inserted on the mesh-generated shaft, which depicts the weight of the crane trolley wheel exerted on the shaft. The weight of the load exerted on the shaft is inspired by the weight of the shaft from real-life which is 30kN. In the other hand, another force is inserted into the mesh-generated shaft which is the torsional force exerted by the rotor. The rotor transmits the torsional force to the mesh-generated shaft via rotational motion at constant velocity. The constant velocity inserted on the mesh-generated shaft by the rotor is also inserted into the mesh-generated shaft as constant rotational velocity.

In order to study the crack initiation and propagation, a local mesh is generated at the location of the shaft where there is a high tendency for the crack to occur. Hence, local meshes are inserted at local specifications relative to the maximum distance between the element and system boundaries. Via further analysis, the crack generated via local mesh can be analysed via continuous propagation when the structure is exposed to fatigue and cyclic loading.

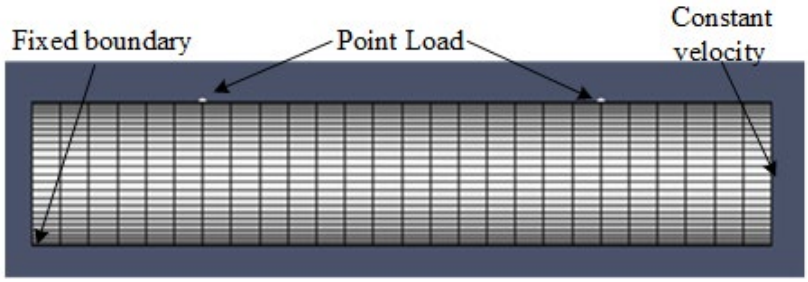

Figure 2.4 The depiction of boundaries condition and loadings on the mesh-generated shaft.

Moreover, several other essential parameters like material properties, crack geometrical characteristics, and fatigue loadings are also emphasised to determine fatigue life prediction. Additionally, via the Finite Element Analysis (FEA) of the local mesh, it also tends to the motion of the fatigue crack propagation process where the crack growth propagation parameters' uncertainty is used to construct the scatter statistics. Hence, the local mesh should be located where there is a high tendency for the crack to occur on the mesh-generated shaft. Based on real-life, the cracks are formed at the downside of the shaft. Hence, the local mesh is inserted in the exact area as the crack in real life which is depicted in Figure 2.5 & 2.6.

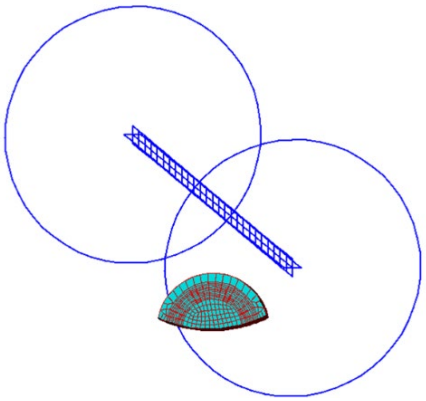

Figure 2.5 Depiction of a local mesh on the outline of the mesh generated shaft.

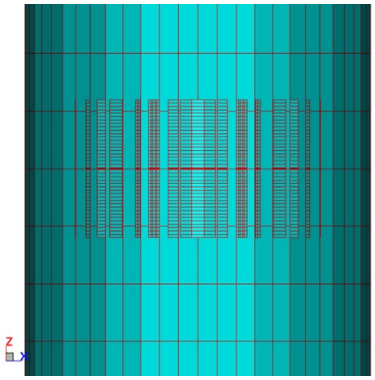

Figure 2.6 Back view depiction of the local mesh on the mesh-generated shaft.

Via the finite element formulation, the software depicts the surface crack growth (crack propagation), where the propagation can be studied and analysed. The crack propagation at the local mesh is created once the boundary conditions and fatigue loading is inserted on the shaft. Depending on the fatigue loading and formulation, the level of crack propagation is created. Each level of crack propagation is classified and categorised as beachmarks. The data propagation of each beackmark is classified into separate files where the data could be used to validate and study the crack propagation. The beackmarks of each level are depicted in Figure 2.7, 2.8, and 2.9.

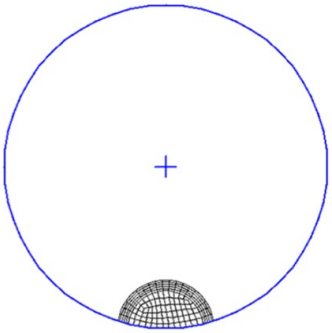

Figure 2.7 Depiction of the 1st beachmark crack propagation

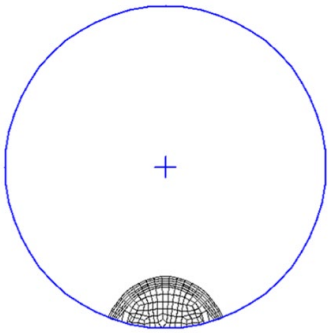

Figure 2.8 Depiction of the 3rd beachmark crack propagation

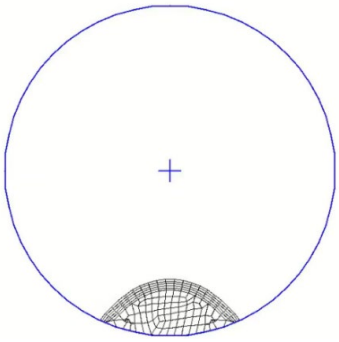

Figure 2.9 Depiction of the 5th beachmark crack propagation

The beachmarks are formed due to mode I loading which causes the cracks to undergo opening mode. In relation, the loads are applied normally to the rotating shaft in constant velocity which causes the shaft to initiate a crack. The mode I loading causes the crack to open and propagate. Most failures in rotor shafts are mainly because Mode I cyclic loadings. Whilst the SIF of a cracked shaft under mode I loading, is given by:

Global equation: $\{F\} = [K]\{\Delta\}$

3 RESULTS & DISCUSSION

The data obtained from the S-FEM Software for each level of beachmarks are used to plot graphs (*y*-axis displacement vs *x*-axis displacement) which the graphs are used to study and analyse the crack propagation of the mesh-generated shaft. Thus, it allows a vivid depiction of the crack propagation from one beachmark level to another. The displacement of nodes (nodal displacement) is adapted to plot the graph, which tenders an illustration of each node from one beachmark level to another. Nodes are points labelled around the parameter of the cracks, used to study the crack propagation. Thus, the nodal displacement plays a significant role in this study. Figures 3.1, 3.2, & 3.3 depict the graph plot (*y*-axis displacement vs *x*-axis displacement) of the nodes at each beachmark level. Moreover, all these graphs have depicted a curvy bell-shaped graph. The obtained data used for the graph plots for each beackmark levels portray the increasing trend of the *y*-axis displacement of nodes till the nodal midpoint, which then the *y*-axis displacement starts to show a decreasing trend till the final node with respect to the increasing *x*-axis displacement of each node. Thus, the data trend tends to be a curvy bell-shaped graph. Moreover, the nodal displacement of each node can be seen to increase significantly with the increasing beachmark levels. For example, the 10th nodal point for each beachmark has higher *x*- and *y*-axis displacement compared to the previous 10th nodal point beackmark level. Thus, the *x*- and *y*-axis displacement for each 10th nodal point beachmarks increases as the increasing beachmark levels.

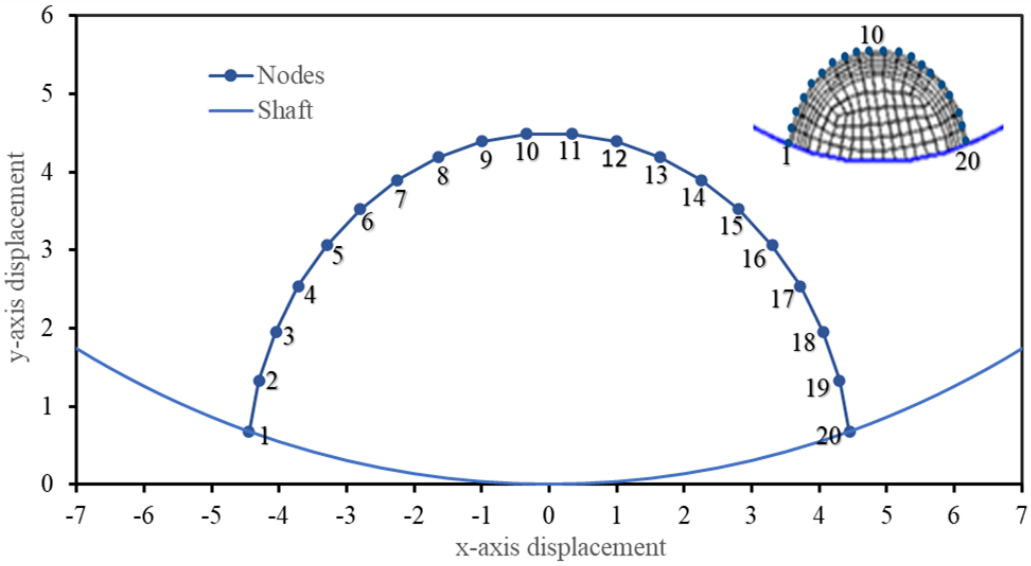

Figure 3.1 Graph plot depiction of the 1st beachmark crack propagation

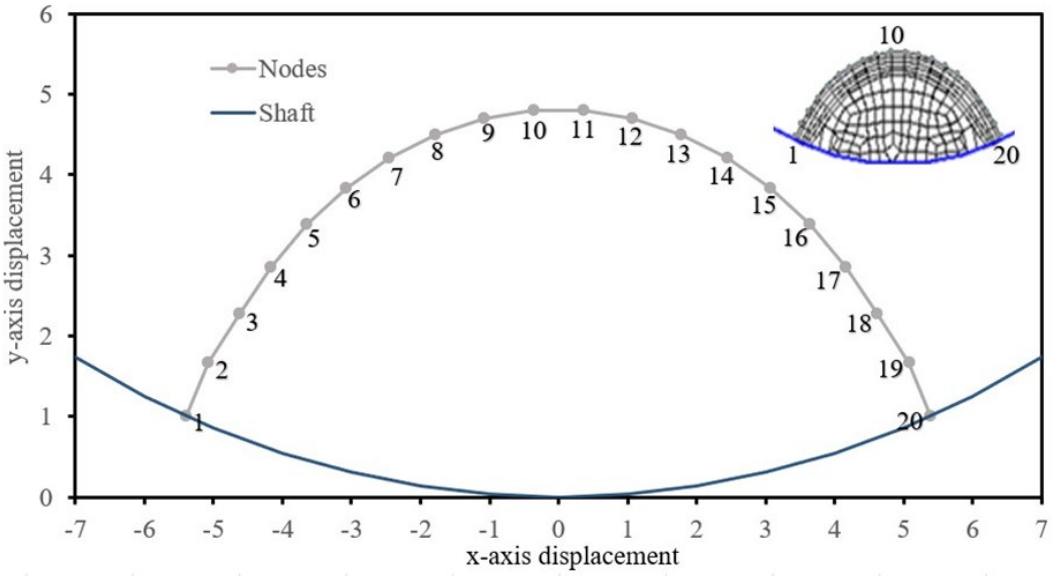

Figure 3.2 Graph plot depiction of the 3rd beachmark crack propagation

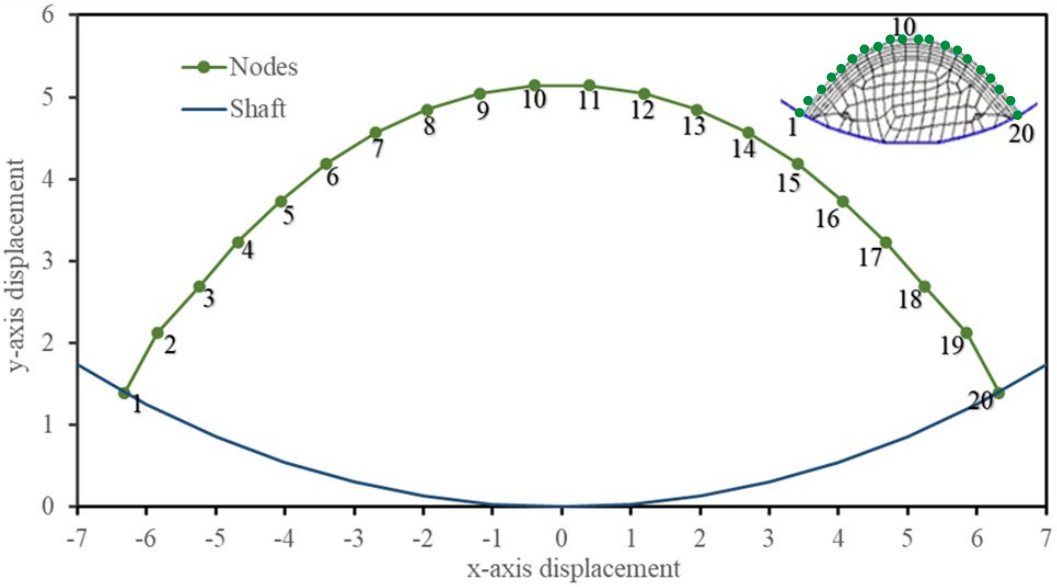

Figure 3.3 Graph plot depiction of the 5th beachmark crack propagation

Moreover, Figure 3.4 depicts the graph plot (*y*-axis displacement vs *x*-axis displacement) for all beackmark levels combined. Meaning that every curvy bell-shaped curve from all beachmark levels is combined into a single graph to study and analyse the rhythm of nodal displacement and crack propagation. Figure 3.4 portrays that the curvy bell-shaped curve for all beachmark levels is seen to have the ideal curvy shape, which increases significantly with the increasing beackmark levels. Thus, it denotes that the curve from the 3rd beachmark level depicts a higher *x*- and *y*-axis displacement than the 1st and 2nd beachmark levels, where a higher curvy bell-shaped curve is obtained compared to the other curves from the 1st and 2nd beachmark levels. Figure 3.4 shows that the nodal displacement for each nodal point increases from one beachmark level to another higher beachmark level.

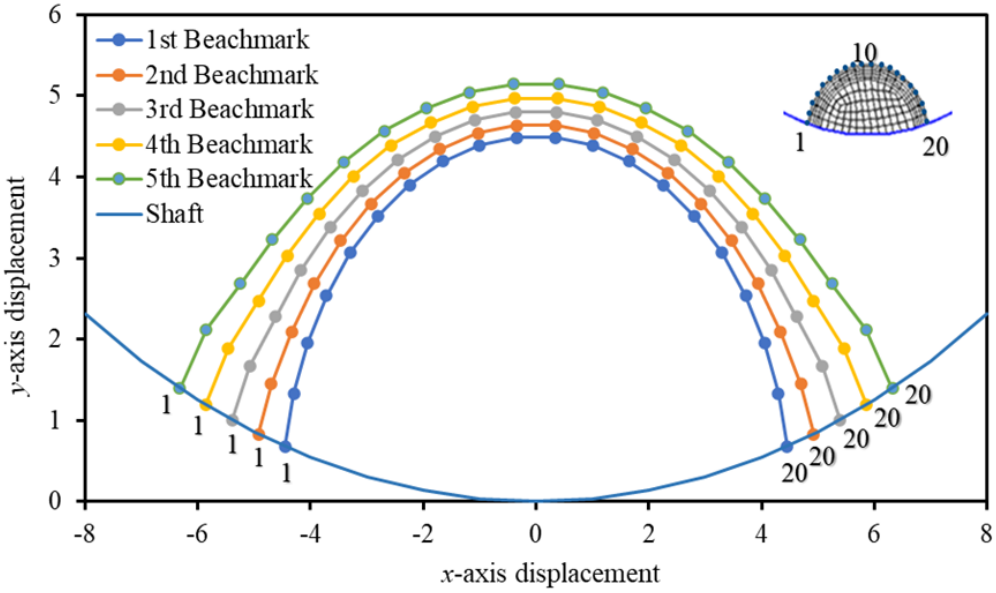

Figure 3.4 Graph plot depiction of all combined beachmarks

In addition, the crack propagation of each beachmark level can also be analysed in term of SIF. SIF is usually used to predict the stress intensity near the crack tip where crack propagation occurs. SIF tenders the information on the stress intensity at the crack tip, which is used to study the propagation of the crack at each level. Moreover, the SIF also renders the crack propagation resistant towards stresses which derives from its ability to overcome stresses subjected to the shaft. The S-FEM software is able to deliver the results of the average SIF at each nodal point of the crack. The average SIF data is obtained regarding each nodal displacement of the cracks, as in **Table 3.1**.

Figure 3.5 depicts the average Stress Intensity Factor (SIF) of the cracked surface on the mesh-generated shaft with combined nodal points of all beachmark levels. The SIF is analysed at the crack tip of the cracked surface. The graph from Figure 3.5 tends a U-shaped graph plotted from the data obtained from the software's file. The U-shaped graph starts with the falling of average SIF from nodal point 1 till it reaches the nodal point with the most petite average SIF. From that particular point, the nodal point with the most petite average SIF (nodal point 7), the graph rises until it reaches the final one with the highest average SIF. The nodal point with the lowest average SIF is seen to be at nodal point 7 with a SIF of 130.16 MPa, and the highest average SIF is said to be at nodal point 20 with an average SIF of 150.76 MPa. The two highest nodal points of all combined beachmark levels can be observed at the 1st and 20th nodal points. In conjunction with the graph plotting, the highest SIF is said to be situated at the nodal points 1 and 20 which means that the stress intensity is higher at that particular nodal area compared to the area perimeter other nodal points. In accordance, the nodes of the local mesh depict an average SIF value higher than the SIF_{IC} which initiates the formation of cracks. The average SIF of the local meshes' perimeter nodes are able to constitute the crack to propagate and enlarge from one beachmark level to another level higher, due to the immense average SIF.

Table 3.1 The data table of nodal displacement and average stress intensity factor (sif) of all combined beachmarks

NODES	**1**	**2**	**3**	**4**	**5**	**6**	**7**	**8**	**9**	**10**
Average Stress Intensity Factor (SIF) of the nodes **(MPa*m$^{1/2}$)**	145.48	139.92	135.84	133.06	131.32	130.41	130.16	130.42	131.09	132.08
NODES	**11**	**12**	**13**	**14**	**15**	**16**	**17**	**18**	**19**	**20**
Average Stress Intensity Factor (SIF) of the nodes **(MPa*m$^{1/2}$)**	133.33	134.80	136.44	138.21	140.11	142.10	144.18	146.32	148.52	150.76

Furthermore, this discussion continues with a more elaborated explanation of the analysis done in the S-FEM software. The S-FEM software is used due to its capability to render an intricate

output which the results is highly beneficial for this study. This study does ‘not only concentrate with the analysis of the crack prone area of the shaft, however, deepens the study towards the simulation of affair on that area, upon the subjection of continuous loading. Upon the subjection of loading, the cracks which were initiated, tends to propagate across the shaft. If the fatigue is enough to propagate the crack to a wise extend, this causes the shaft to undergo plastic deformation and eventually may lead to complete fracture upon the continuous cyclic loading. Thus, the S-FEM software is used to simulate the growth of fatigue cracks on the shaft to study its response towards cyclic loading as in Table 3.1. The S-FEM software tenders its capability to deliver a crack propagating mechanism via the generation of local mesh. Thus, the local mesh needs to be generated so that the crack growth and propagation simulation can be conducted. The simulation and analysis of crack growth and propagation can only be done with the use of a sophisticated software; thus, the S-FEM software is used.

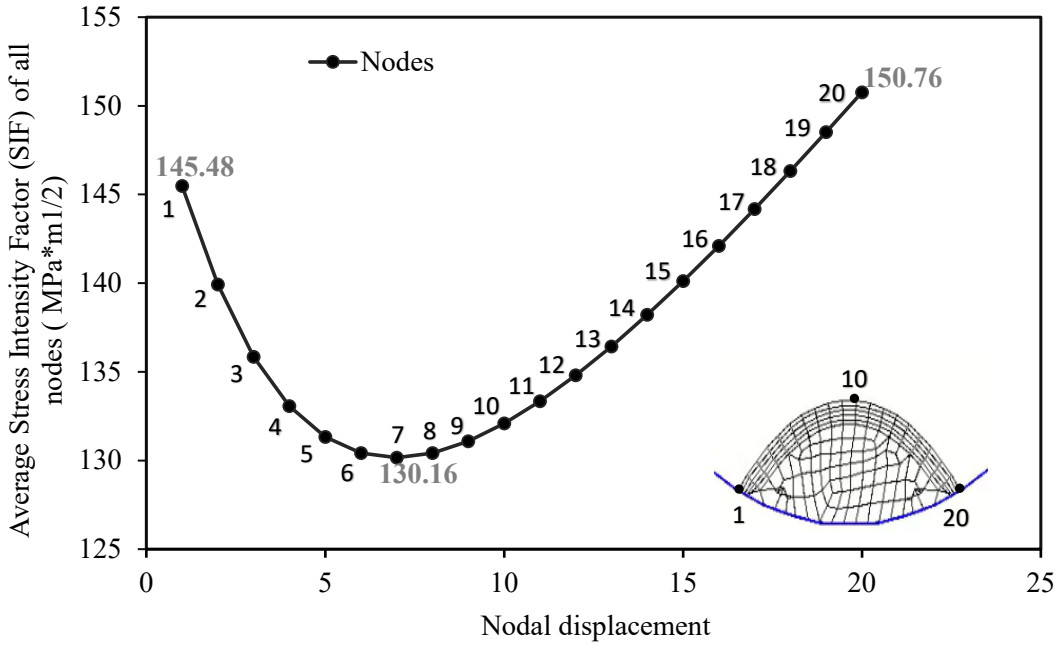

Figure 3.5 Graph plot depiction of average stress intensity factor (SIF) of all combined beachmarks

4 CONCLUSION

The SIF obtained at the crack tips are higher compared to the SIF_{IC} (40-50 MPa.m^2 for 4140 alloy steel), which is the foremost reason for the formation and propagation of cracks. The

results showed the predicted crack propagation and SIF calculation is crucial for maintenance preceding and retirement of the structure.

ACKNOWLEDGMENTS

The author would like to acknowledge the Ministry of Higher Education under Fundamental Research Grant Scheme FRGS/1/2023/TK03/UMP/02/26 (university reference RDU230134) and Universiti Malaysia Pahang Al-Sultan Abdullah (UMPSA) for financial support RDU220367.

REFERENCES

[1] N. Winzer, C. Bischoff, P. Brugger, and I. Thomas, "Factors influencing the resistance of dual-phase steels to edge cracking," *Materials Science and Engineering: A*, vol. 880, p. 145334, 2023, doi: https://doi.org/10.1016/j.msea.2023.145334.

[2] H. Yang, Y. Sheng, J. Zhang, W. Ma, and X. Jiang, "The influenced zones of stress intensity factor and plasticity at multi-crack tips," *Theoretical and Applied Fracture Mechanics*, vol. 127, p. 103978, 2023, doi: https://doi.org/10.1016/j.tafmec.2023.103978.

[3] A. Yosri, A. Zayed, S. Saad-Eldeen, and H. Leheta, "Influence of stress concentration on fatigue life of corroded specimens under uniaxial cyclic loading," *Alexandria Engineering Journal*, vol. 60, no. 6, pp. 5205–5216, 2021, doi: https://doi.org/10.1016/j.aej.2021.04.004.

[4] J. Wu, H.-Z. Huang, Y.-F. Li, S. Bai, and A.-D. Yu, "Probabilistic fatigue life prediction of an aero-engine turbine shaft," *Aircraft Engineering and Aerospace Technology*, vol. 94, no. 10, pp. 1854–1871, 2022, doi: 10.1108/AEAT-08-2021-0232.

[5] J. Wu, H.-Z. Huang, Y.-F. Li, S. Bai, and A.-D. Yu, "Probabilistic fatigue life prediction of an aero-engine turbine shaft," *Aircraft Engineering and Aerospace Technology*, vol. 94, no. 10, pp. 1854–1871, 2022, doi: 10.1108/AEAT-08-2021-0232.

[6] S. Bai, Y.-F. Li, H.-Z. Huang, Q. Ma, and N. Lu, "A probabilistic combined high and low cycle fatigue life prediction framework for the turbine shaft with random geometric parameters," *Int J Fatigue*, vol. 165, 2022, doi: 10.1016/j.ijfatigue.2022.107218.

[7] M. R. M. Akramin, A. Alshoaibi, M. S. A. Hadi, A. K. Ariffin, and N. A. N. Mohamed, "Probabilistic analysis of linear elastic cracked structures," *Journal of Zhejiang University: Science A*, vol. 8, no. 11, 2007, doi: 10.1631/jzus.2007.A1795.

[8] J. Zhang, W. Y. Liu, Q. Z. Zhu, and J. F. Shao, "A novel elastic–plastic damage model for rock materials considering micro-structural degradation due to cyclic fatigue," *Int J Plast*, vol. 160, p. 103496, 2023, doi: https://doi.org/10.1016/j.ijplas.2022.103496.

[9] A. Zorman, J. Slavič, and M. Boltežar, "Vibration fatigue by spectral methods—A review with open-source support," *Mech Syst Signal Process*, vol. 190, p. 110149, 2023, doi: https://doi.org/10.1016/j.ymssp.2023.110149.

[10] M. R. M. Akramin, M. S. Shaari, A. K. Ariffin, M. Kikuchi, and S. Abdullah, "Surface crack analysis under cyclic loads using probabilistic S-version finite element model," *Journal of the Brazilian Society of Mechanical Sciences and Engineering*, vol. 37, no. 6, 2015, doi: 10.1007/s40430-015-0416-3.

[11] A. Bovsunovsky, E. Shtefan, and V. Peshko, "Modeling of the circumferential crack growth under torsional vibrations of steam turbine shafting," *Theoretical and Applied Fracture Mechanics*, vol. 125, p. 103881, 2023, doi: https://doi.org/10.1016/j.tafmec.2023.103881.

[12] P. Li *et al.*, "A review on phase field models for fracture and fatigue," *Eng Fract Mech*, vol. 289, p. 109419, 2023, doi: https://doi.org/10.1016/j.engfracmech.2023.109419.

[13] M. M. N. Husnain, M. R. M. Akramin, M. S. Shaari, A. Takahashi, A. H. Bashiri, and A. M. Alshoaibi, "Comparison of Monte Carlo and bootstrap analyses for residual life and confidence interval," *Materials Science-Poland*, vol. 41, no. 1, pp. 15–26, 2023, doi: doi:10.2478/msp-2023-0003.

[14] S. K. Suman and R. Dwivedi, "Surface crack and fatigue analysis for cylindrical shaft," *Mater Today Proc*, vol. 47, pp. 6211–6219, 2021, doi: https://doi.org/10.1016/j.matpr.2021.05.161.

[15] O. Elmhaia, Y. Belaasilia, O. Askour, B. Braikat, and N. Damil, "Numerical analysis of frictional contact between crack lips in the framework of Linear Elastic Fracture Mechanics by a mesh-free approach," *Theoretical and Applied Fracture Mechanics*, vol. 124, p. 103749, 2023, doi: https://doi.org/10.1016/j.tafmec.2023.103749.

[16] P. Rubio, J. Bernal, B. Muñoz-Abella, and L. Rubio, "A closed expression for the Stress Intensity Factor of concave fatigue cracks in rotating shafts," *Eng Fract Mech*, vol. 214, pp. 233–247, 2019, doi: https://doi.org/10.1016/j.engfracmech.2019.02.034.

[17] P. Rubio, Y. Sanz, L. Rubio, and B. Muñoz-Abella, "Stress Intensity Factor and propagation of an open sickle shaped crack in a shaft under bending," *Theoretical and Applied Fracture Mechanics*, vol. 96, pp. 688–698, 2018, doi: https://doi.org/10.1016/j.tafmec.2017.10.008.

[18] P. Rubio, L. Rubio, B. Muñoz-Abella, and L. Montero, "Determination of the Stress Intensity Factor of an elliptical breathing crack in a rotating shaft," *Int J Fatigue*, vol. 77, pp. 216–231, 2015, doi: https://doi.org/10.1016/j.ijfatigue.2015.01.018.

[19] A. J. Pachoud, P. A. Manso, and A. J. Schleiss, "Stress intensity factors for axial semi-elliptical surface cracks and embedded elliptical cracks at longitudinal butt welded joints of steel-lined pressure tunnels and shafts considering weld shape," *Eng Fract Mech*, vol. 179, pp. 93–119, 2017, doi: https://doi.org/10.1016/j.engfracmech.2017.04.024.

[20] M. R. M. Akramin, M. S. Marizi, M. N. M. Husnain, and M. Shamil Shaari, "Analysis of Surface Crack using Various Crack Growth Models," in *Journal of Physics: Conference Series*, 2020. doi: 10.1088/1742-6596/1529/4/042074.

[21] M. H. Mohd Noh, M. A. Mohd Romlay, C. Z. Liang, M. S. Shaari, and A. Takahashi, "Analysis of stress intensity factor for fatigue crack using bootstrap S-version finite element model,"

International Journal of Structural Integrity, vol. 11, no. 4, pp. 579–589, 2020, doi: 10.1108/IJSI-10-2019-0108.

[22] M. R. M. Akramin, A. K. Ariffin, M. Kikuchi, and S. Abdullah, "Sampling method in probabilistic S-version finite element analysis for initial flaw size," *Journal of the Brazilian Society of Mechanical Sciences and Engineering*, vol. 39, no. 1, 2017, doi: 10.1007/s40430-016-0549-z.

[23] M. S. Shaari, M. R. M. Akramin, A. K. Ariffin, S. Abdullah, and M. Kikuchi, "Prediction of fatigue crack growth for semi-elliptical surface cracks using S-version fem under tension loading," *Journal of Mechanical Engineering and Sciences*, vol. 10, no. 3, 2016, doi: 10.15282/jmes.10.3.2016.14.0220.

[24] S.-P. Zhu, W.-L. Ye, J. A. F. O. Correia, A. M. P. Jesus, and Q. Wang, "Stress gradient effect in metal fatigue: Review and solutions," *Theoretical and Applied Fracture Mechanics*, vol. 121, p. 103513, 2022, doi: https://doi.org/10.1016/j.tafmec.2022.103513.

[25] M. Ozturk, F. Husem, I. Karademir, E. Maleki, A. Amanov, and O. Unal, "Fatigue crack growth rate of AISI 4140 low alloy steel treated via shot peening and plasma nitriding," *Vacuum*, vol. 207, p. 111552, 2023, doi: https://doi.org/10.1016/j.vacuum.2022.111552.